In: "Application of high magnetic fields in semiconductor physics" ed. G. Landwehr (Lecture Notes in Physics, Springer Verlag, Berlin, Heidelberg, New York, Tokio, 1983)

PHASE TRANSITIONS IN HIGH MAGNETIC FIELDS

A.J. Arko[a], C.J. Beers, A.P.J. van Deursen, R.P.A.R. van Kleef, H.W. Myron, M.R. Parker[b], M. Pepper[c], D.A. Poole[c], Th.H.M. Rasing and P. Wyder
High Field Magnet and Physics Laboratory, Faculty of Science
University of Nijmegen
Toernooiveld, 6525 ED Nijmegen, The Netherlands

a) Material Science Division
Argonne National Laboratory
Argonne, Illinois, U.S.A.

b) Department of Pure and Applied Physics
University of Salford
Salford, England

c) Cavendish Laboratory
Cambridge University
Cambridge, England

The purpose of this paper is to summarize some of the research activities recently performed at the Laboratorium voor Hoge Magneetvelden at the University of Nijmegen. The scope here and unifying aspect is magnetically induced phase transitions. Here we summarize transitions in the settling velocity of paramagnetic aggregates, suppression of spin fluctuations in UAl_2, the phase diagram of a ferroelectric chiral smectic liquid crystal near the Lifshitz point and the transition from 3D to 2D conduction in a GaAs FET. In no way does this represent a complete review of transitions, but rather a summary of phase transitions observed at the magnet laboratory during the past year.

Magnetic Aggregation of Particles in High Fields

The stability of a colloidal suspension of particles is generally described by the Derjaguin-Landau-Verwey-Overbeek (DLVO) theory [1] where the two particle potential energy ϕ_T can be expressed by the sum of potential energy ϕ_R, due to the electrical double layers at the solid-liquid interface, and a London-van der Waals interaction term, ϕ_L. These interactions for particles of equal radii are given respectively by:

$$\Phi_R = 4\pi\epsilon_r\epsilon_0 a\psi_0^2 \frac{\exp[-\tau(r_a-2)]}{r_a} \qquad (1)$$

and

$$\Phi_L = -\frac{A}{6}\left[\frac{2}{r_a^2-4} + \frac{2}{r_a^2} + \ln\left(\frac{r_a^2-4}{r_a^2}\right)\right] \qquad (2)$$

where ϵ_r is the relative permittivity of the material of the particle, ϵ_0 the permittivity of free space, ψ_0 the double layer potential, $r_a = r/a$ the normalized interparticle distance (a particle size) and τ/a is the Debye-Hückel reciprocal double layer thickness. A potential energy barrier exists in a stable suspension which prevents the particles from approaching each other. The DLVO-theory can be extended [2] when an external magnetic field B_0 is turned on and the dipole-dipole interaction energy Φ_M is included. For a system of two particles, Φ_M is

$$\Phi_M = -\frac{32\pi^2 a^3 \chi^3 B_0^2}{9\mu_0 r_a^3}, \qquad (3)$$

where μ_0 is the permeability of free space and χ is the net volume magnetic susceptibility of the particle. The total potential energy of interaction is given by the sum of Eqs. 1 to 3 and since Φ_M is negative, an applied magnetic field can reduce the potential energy to zero thereby allowing the particles to approach each other and form binary clusters.

In order to understand the dynamics of flocculation, a force balance equation can be constructed from the spatial derivatives of Φ_R, Φ_L and Φ_M [3]. Fixing a polar coordinate system at the center of the first particle and the direction of the applied magnetic field parallel to the x-axis, the dynamics of the radial and azimuthal components of the second are respectively given by:

$$\frac{dr_a}{dt} = - V_{Ma} \left(\frac{3\cos^2\theta - 1}{r_a^4} \right) + V_{La} \left[\frac{2}{r_a(r_a^2-4)} - \frac{r_a}{(r_a^2-4)^2} - \frac{1}{r_a^3} \right] + V_{Ra} \left(\frac{\tau r_a + 1}{r_a^2} \right) \exp\left[-\tau(r_a - 2) \right] \tag{4}$$

$$r_a \frac{d\theta}{dt} = - V_{Ma} \frac{\sin 2\theta}{r_a^4} \tag{5}$$

Here V_{Ma}, V_{La} and V_{Ra} are normalized characteristic velocity coefficients analogous to the magnetic velocity used in HGMS.

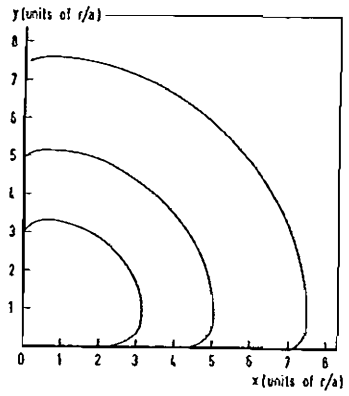

Fig. 1 Particle trajectories in a paramagnetic flocculation process with an external magnetic field B_0 along the x-axis. The initial angular position of the particles is at $\theta = 89^0$.

Using a forth order Runge-Kutta technique, particle trajectories have been calculated from Eqs. 5 and 6 and are shown in Fig. 1. A paramagnetic particle initially positioned at a point (r,θ) in the first quadrant, precesses clockwise about the "fixed" particle at the origin. If the particle is captured it moves along the x-axis towards the point (2a,0) forming a binary pair. For particles located at a distance greater than r_{ca}, the normalized capture radius, the particle is pushed away along the x-axis.

The capture radius r_{ca} can be estimated to a very good approximation, if θ is set equal to zero in Eqs. 4 and 5. Neglecting the London-van der Waals interaction and assuming τ is small, then the capture radius $r_{ca} = (2\ V_M/V_R)^{\frac{1}{2}}$. From the capture radius one can estimate the particle number density at which flocculation can be expected to be observed. This is of the order of

$$n_0 = \left(\frac{3}{8 \cdot 4\pi a^3} \right) (V_R/V_M)^{3/2}$$

Flocculation experiments were carried out on a number of commercially available mineral suspensions. The magnetic fields were produced by a water cooled Bitter magnet. Suspensions of paramagnetic materials were held in calibrated testtubes in the magnet. Field induced particle aggregation was detected by measuring the settling velocity V_s of the suspended particle at different values of the applied magnetic field. This was achieved by optically measuring the rate of fall of the meniscus between sedimenting particles and clear liquid using a cathetometer or videocamera.

The settling process can be described by a simple force balance equation between the dragforce and the combined influence of the gravitational and magnetic dipole forces:

$$\frac{4\pi}{3} a^3 \rho_{eff} g + \frac{4}{3} \pi a^3 \chi_{eff} \xi B_0^2/\mu_0 = 6\pi\eta a V_s \qquad (6)$$

where ρ_{eff} is the effective density of the particle in the fluid, χ_{eff} is the net volume susceptibility, ξ is the fractional magnitude of the field gradient and η is the viscosity of the carrier fluid. When the magnetic field exceeds B_F two-particle clusters are formed which will align along the field direction, as shown in Fig. 1. With a vertical magnetic field this means that the Stoke's drag term on the RHS of Eq. 6 will remain relatively unaffected since the effective airodynamic diameter of the cluster will not be very different from that of the single particle. On the other hand, the volume dependent term on the LHS of Eq. 6 will double in size. We expect that the settling velocity plotted against B_0^2 will change discontinuously at $B_0 = B_F$ whereas its slope should approximately double.

Fig. 2.

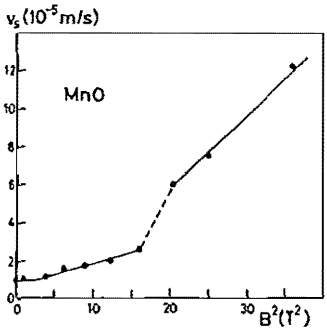

a) Settling velocity of a 30%-vol suspension of MnO in a vertical magnetic field. The discontinuity of V_s vs. B^2 indicates pair formation of particles. The volume susceptibility (MKSA units) is $\chi = 4.69 \times 10^{-3}$

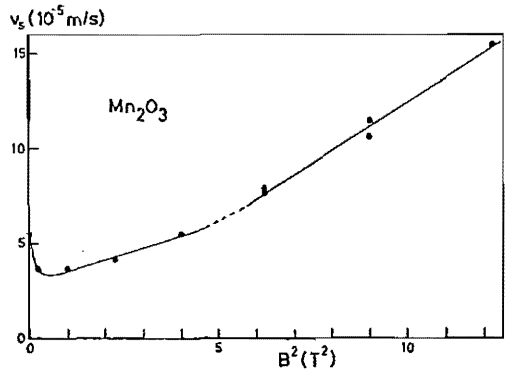

b) V_s in a 25%-vol suspension of Mn_2O_3. χ(MKSA) = 5.39×10^{-3}.

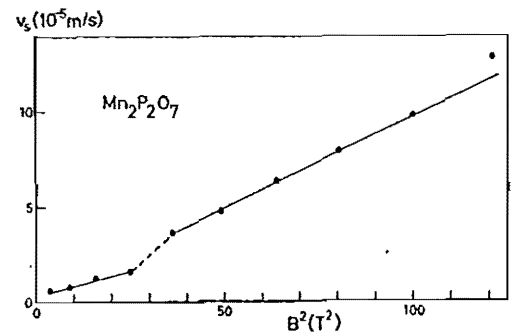

c) V_s in a 35%-vol suspension of $Mn_2P_2O_7$. χ(MKSA) = 4.72×10^{-3}.

Measurements of settling velocity as a function of field were carried out on MnO, Mn_2O_3 and $Mn_2P_2O_7$. Fig. 2 shows field induced binary flocculation for Mn_2O_3 and $Mn_2P_2O_7$. In the case of MnO the slope changes by more than a factor of two; this is not clearly understood. The minimum at low fields in Mn_2O_3 is thought to be caused by a combination of two effects: an anisotropic magnetic susceptibility and a nonspherical particle shape. Particles rotate that their strongest magnetic axis is directed parallel to the field, thus altering their effective diameter.

Suppression of Spin Fluctuations in UAl_2 in High Magnetic Fields

UAl_2 has been known for some time to be a spin-fluctuation (SF) system. Its temperature dependence of specific heat, resisitivity and magnetic susceptibility [4] fit neatly into various theories explaining these phenomena [5]. The characteristic SF temperature (T_{SF}) of UAl_2 is believed to be about 25 K. We have studied the transport properties of UAl_2 at low temperatures in high magnetic fields [6] where it has been argued that the application of high magnetic fields will reduce or freeze out paramagnon effects. The Zeeman splitting of the spin-up and spin-down electron states will prevent certain excitations with the reversal of spin direction to occur. The characteristic paramagnon excitations are of the order of k_BT_{SF}, with g = 2. The relationship between H_{SF} and T_{SF} (25 K) can be written as $g\mu_BH_{SF} = k_BT_{SF}$. H_{SF} is then calculated to be near 19 T.

Partial freezing out of SF in high magnetic fields has been previously reported for various compounds, for example in Pd [7] H_{SF} is believed to be 190 T! In contrast we have achieved complete suppression of SF in UAl_2.

The susceptibility of UAl_2 [6], derived from the magnetization at 1.4 and 4.2 K, decreases with increasing field reaching a field-independent value above 20 T. At 20 and 77 K the susceptibility is found to be independent of magnetic field. Values for the differential susceptibility, see Table I, for various field intervals as a function of temperature indicate that the high-field values at 4.2 and 1.4 K correspond to the low-field values of Brodsky and Trainor at 25 K.

Table I Molar susceptibilities of UAl_2. The units of $\frac{\partial M}{\partial H}$ are 10^{-9} m^3/mole.

T(K)	$\frac{\partial M}{\partial H}$ (1.5 T)	$\frac{\partial M}{\partial H}$ (2 - 5 T)	$\frac{\partial M}{\partial H}$ (20 - 35 T)
1.4	-	56.5	47.3
4.2	55.0	55.4	47.3
20	-	47.7	47.7
25	47.3	-	-
50	46.6	-	-
77	45.5	45.9	45.9

a) Ref. 4 - Brodsky and Trainor.

The temperature and field dependence of the magnetic susceptibility suggest that an equivalent contribution can be suppressed either by applying a magnetic field of about 20 T or increasing the temperature to T_{SF}.

The temperature dependent susceptibility has also been measured from 4.2 to 270 K at 1,2 and 8.0 T. The low temperature data corresponds to an expression $\chi = \chi_0 (1 - T^2/T_{SF}^2)$. The change of the specific heat in a magnetic field can be predicted from the susceptibility through the Maxwell relation,

$$\left(\frac{\partial S}{\partial \mu_0 H} \right)_{T,p} = \left(\frac{\partial M}{\partial T} \right)_{H,p} \qquad (7)$$

On taking the temperature derivative and using $M = \chi H$, we find that

$$\left(\frac{\partial C_p}{\partial \mu_0 H}\right) = TH\left(\frac{\partial^2 \chi}{\partial T^2}\right)_{H,p} \tag{8}$$

Since the electronic contribution to the specific heat is linear in temperature and using the T^2 fit to the susceptibility, we find that Eq. 8 can be written as

$$\left(\frac{\partial \gamma}{\partial \mu_0 H}\right) = -2H\left(\chi_0/T_{SF}^2\right)_{H,p} \tag{9}$$

From Table I, χ_0 decreases with increasing field thus the specific-heat coefficient γ diminishes with a power law less than H^2. The specific heat experiments by Trainor et al. [4] are in very good agreement with the suppression of $\Delta\gamma/\gamma$ calculated here to be -1.25% at 4 T.

The magnetoresistance shows a bending over at fields of about 15 T, as shown in Fig. 3. The power law is $\frac{\Delta\rho}{\rho} = H^n$; for fields between 0 and 15 T, n = 1.45, while above 15 T, n = 1.3. Hertel, Appel and Fay [8] calculated the magnetic field dependence of UAl_2 where a 14% suppression of the SF contribution is predicted at 10 T. If we assume that the magnetoresistance due to paramagnons and other effects (band, e - e, e - p, etc.) are in series then the total resistivity may be written as $\Delta\rho = \Delta\rho_{SF} + \Delta\rho_{other}$. If we additionally assume that ρ_{SF} is maximum at zero field (contributing 30% at H = 0, from an extrapolation above 15 T) then the paramagnon contribution is suppressed by 75% at 10 T.

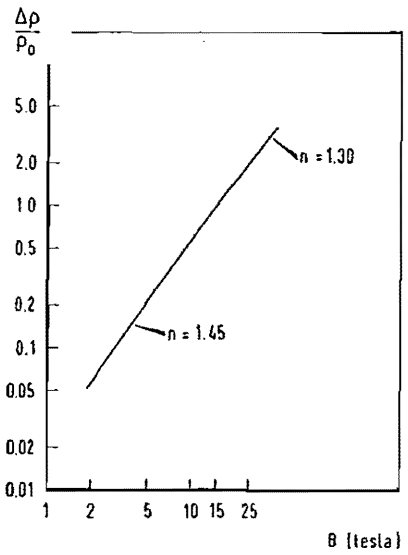

Fig. 3 Magnetoresistivey of UAl_2 at 4.2 K.

We find that the paramagnon effects at low temperature in UAl_2 are large and are frozen or suppressed in fields above H_{SF}. The characteristic field and temperature are related by $g\mu_B H_{SF} = k_B T_{SF}$, with g = 2. As a result of suppression of SF (above H_{SF}) it is quite plausible that the de Haas-van Alphen effect can only be seen when all paramagnon contributions to the effective mass are frozen out. In preliminary experiments, dHvA oscillations have been observed in UAl_2 only above 20 T [9]. In addition, these experiments suggest that field and temperature effects on the paramagnon contributions to the transport properties are closely related.

Magnetic Phase Diagram of a Ferroelectric Chiral Smectic Liquid Crystal near the Lifshitz Point

The Lifshitz point [10] is that point on a line of second-order phase transitions where an instability occurs in wave vector space. It represents a special case of a triple point between a disordered, homogeneously ordered ($\vec{k} = 0$), and modulated phase ($\vec{k} \neq 0$). It has been predicted [11] that a Lifshitz point exists in the T - H phase diagram of chiral smectic liquid crystals if the magnetic field is applied parallel to the smectic layers.

Here the phase diagram of the chiral ferroelectric smectic liquid crystal p-decyloxybenzilidene-p'-amino-2-methybutyl cinnamate (DOBAMBC) is presented [12] which suggests that a Lifshitz point exists between the disordered smectic-A, the helicoidally ordered smectic-C*, and the homogeneously ordered smectic-C phases. The observed T_c - H phase diagram in magnetic field up to 14.5 T is shown in Fig. 4. The A - C* line was found to be of second order whereas the C - C* transition line is of first order close to the λ line. The discontinuity in $\vec{k}$ becomes smaller as the Lifshitz point is approached along the C* - C boundary. Above H = 8.5 T the C - C* line changes its direction so that a reentrant smectic-C* phase was found.

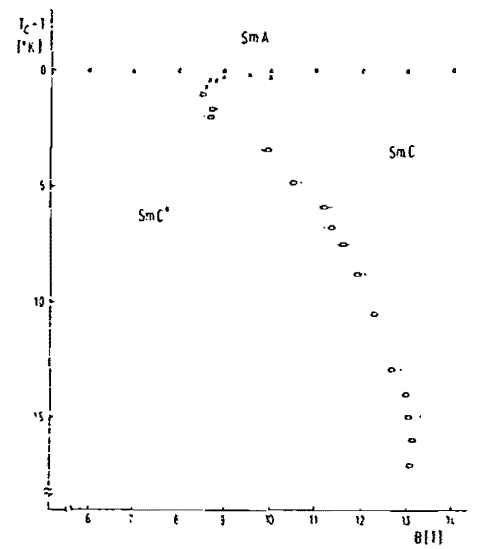

Fig. 4 Phase diagram of chiral DOBAMBC near the smectic A - C* - C triple point. The magnetic field H is applied parallel to smectic layer.

The temperature and magnetic field dependence of the in-plane component of the dielectric constant ϵ and the pitch $2\pi/k$ of the smectic-C* helix were measured in order to determine the phase boundaries. Simultaneous dielectric and optical measurements were performed using optically flat glass plates with transparent SnO_2 electrodes. The molecules were oriented parallel to the cell walls by slowly cooling (1°C/h) the system through the isotropic-smectic A transition in a magnetic field of 10 T. The C - C* phase boundary and the critical magnetic field H_c for unwinding the smectic-C* helix was determined by measuring $\epsilon = \epsilon(H)$ at T = const. The sweep rate was 1.45 T/min. The A - C* boundary was determined by measuring $\epsilon = \epsilon(T)$ at H = const.

The inverse pitch $(\vec{k}/\pi)$ must tend to zero as the Lifshitz point is approached. If not, the $\vec{k}$ of the C - C* transition is discontinuous at the A - C* - C triple point. The magnetic field dependence of the wave vector of the C* helix along the λ line has been given [2] as

$$k_\lambda^2(H) = k_0^2(1 - H^4/H_L^4) \quad , \quad H < H_L \tag{10}$$

while $k_\lambda = 0$ for $H > H_L$. Fig. 5 shows k measured as a function of H for constant T. The discontinuity at the C* - C transition decreasing with increasing T as the Lifshitz point is approached. The isotherm ($T_c - T = 0.2$) can be reasonably fit by Eq. 10 with $H_L = 10.2$ T. However, for $T_c - T = 0.1$, H_L is larger than 14 T. The system behaves in the way predicted [2] for $T_c - T > 0.2$, however, for $T_c - T < 0.2$ the critical field for unwinding the helix strongly increases with increasing temperature.

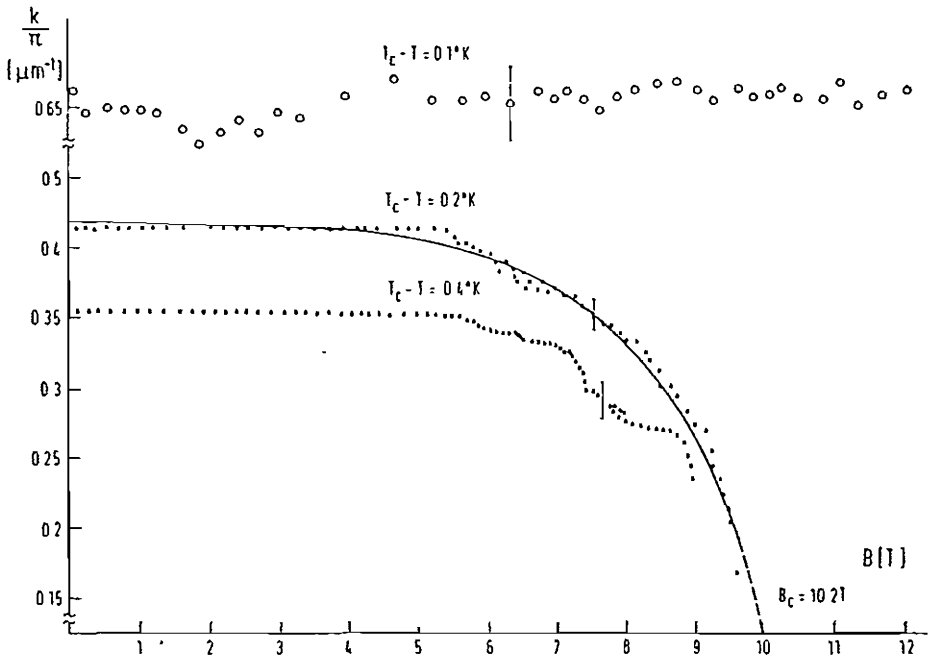

Fig. 5 Magnetic field dependence of the inverse pitch for various temperatures. The solid line through the $T_c - T = 0.2$ K is Eq. 10 with $H_L = 10.2$ T.

Transition from 3D to 2D Conduction in a GaAs-FET

It has been previously suggested [13] that it is possible to achieve a transition from a 3D to quasi 2D electron conduction in a GaAs field effect transistor (FET) by reducing the channel thickness with the gate bias V_g. In the hopping regime this occurs when the hopping distance is close to the channel thickness. In the metallic regime the electron motion perpendicular to the channel is confined to a narrow potential well, motion along the channel remains free electron like. The 3D density of states splits up into discrete sub-bands with only the ground state sub-band being occupied (2D limit) as t tends to zero. For large t, E_F should remain constant (3D limit) and fall for small t when electrons are removed from the channel (2D limit); finally E_F goes to zero at t = 0.

Four experimental measurements were made on each device [14] capacitance, resistance, Hall effect and Shubnikov-de Haas effect. The doping concentration N_D could then be independently confirmed from the capacitance measurements on one hand and the SdH and Hall effect on the other. SdH oscillations for various V_g's with constant substrate voltages were measured and from the periodicity of their oscillations, the Fermi energy is readily determined from

$$n_L = \frac{m^* E_F}{\hbar e B} - \frac{1}{2} \qquad (11)$$

where n_L is the Landau level index. For the device with a doping concentration of $N_D = 2 \times 10^{17}$ cm^{-3}, the Fermi energy is plotted in Fig. 6. From the oscillatory part of the magnetoresistance

$$\cos\left(\frac{2\pi(E_F - E_n)}{\hbar\omega} - \alpha\right) \qquad (12)$$

each sub-band contributes a periodicity dependent on $\Delta E_n = E_F - E_n$. The theoretical oscillation periodicity obtained from Eq. 12 was used to calculate the sub-band energies in Fig. 6 [14]. As t is decreased towards zero it will eventually become less than the mean donor separaration $\bar{r}$ which is 174 Å. A transition from metallic behaviour was observed via the quenching of SdH oscillations for values of $t \simeq \bar{r}$. It can be seen, in Fig. 6, that there is a reasonable agreement between the experimental points and the theoretical predictions for E_F. The fall in E_F as the conducting electron gas in a GaAs FET is confined is confirmed resulting from a 3D to 2D transition.

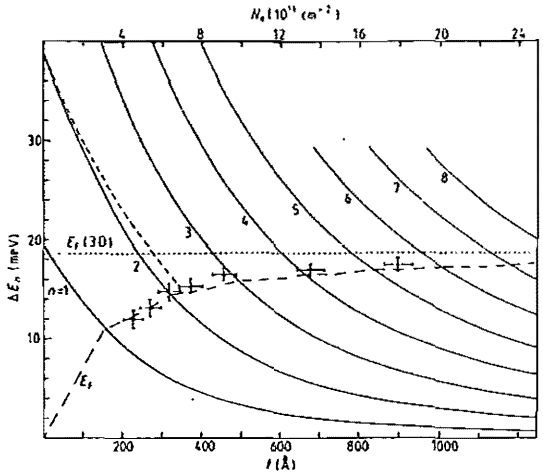

Fig. 6 Level quantization and E_F as a function of channel thickness (t) in a $N_D = 2 \times 10^{17}$ cm^{-3} device. Solid curves are WKB level separation (see ref. 14) ΔE_n and the chain curve to the corresponding E_F. The straight horizontal broken line is E_F (3D) for a uniform non-interacting gas. Measured E_F values are presented as full circles with error bars.

Here we have presented a variety of magnetically induced phase transitions measured at the High Field Magnet Laboratory of the University during this past year. The extent to which magnetic fields help us understand the properties of matter remains significant.

Acknowledgments

We would like to thank Klaas van Hulst, Henk Muileman and Jos Rook of the Nijmegen Magnet Laboratory for their valuable assistance and technical support of this research. Part of this work has been supported by the "Stichting voor Fundamenteel Onderzoek der Materie" (FOM) with financial support of the "Nederlandse Organisatie voor Zuiver Wetenschappelijk Onderzoek " (ZWO).

References

1. E.J.W. Verwey and J.Th.G. Overbeek, Theory of the Stability of Lyophobic Colloids, Elsevier, Amsterdam, 1948.
2. J. Svoboda, Int. J. of Mineral Processing 8, 377 (1981).
3. A more complete discussion can be found in M.R. Parker, R.P.A.R. van Kleef, H.W. Myron and P. Wyder, J. Magn. Magn. Mat. (to be published).

4. R.J. Trainor, M.B. Brodsky and H.V. Culbert, Phys. Rev. Lett. 34, 1019 (1975); A.J. Arko, M.B. Brodsky and W.J. Nellis, Phys. Rev. B 5, 4564 (1972); M.B. Brodsky and R.J. Trainor, Physica 91B, 271 (1977).
5. W.F. Brinkman and S. Engelsberg, Phys. Rev. 109, 417 (1968); A.B. Kaiser and S. Doniach, Int. J. Magn. 1, II (1970); M.T. Béal-Monod, S.K. Ma, and D.R. Fredkin, Phys. Rev. Lett. 20, 750 (1968).
6. For a more extensive report on this phenomena see: J.J.M. Franse, P.H. Frings, F.R. de Boer, A. Menovsky, C.J. Beers, A.P.J. van Deursen, H.W. Myron and A.J. Arko, Phys. Rev. Lett. 48, 1749 (1982).
7. I.Y. Hsiang, J.W. Reister, H. Weinstock, G. Crabtree, and J.J. Vuillemin, Phys. Rev. Lett. 47, 523 (1981).
8. P. Hertel, J. Appel, and D. Fay, Phys. Rev. B 22, 534 (1980).
9. A.J. Arko and J.E. Schirber, J. Phys. (Paris) Colloq. 40, C4 - 9 (1979).
10. R.M. Hornreich, M. Luban, and S. Shtrikman, Phys. Rev. Lett. 35, 1678 (1975).
11. A. Michelson, Phys. Rev. Lett. 39, 464 (1977).
12. For a more complete description of this work see: I. Muševič, B. Žekš, R. Blinc, Th. Rasing and P. Wyder, Phys. Rev. Lett. 48, 192 (1982).
13. M. Pepper, J. Phys. C 10, L173 (1977).
14. For a more complete description see: D.A. Poole, M. Pepper, K.-F. Berggren, G. Hill and H.W. Myron, J. Phys. C 15, L21 (1982).